Analyst

Accepted Manuscript

ROYAL SOCIETY OF CHEMISTRY

www.rsc.org/analyst

Electroanalysis of As(III) at nanodendritic Pd on PEDOT

Sthitaprajna Dash and N. Munichandraiah*

Department of Inorganic and Physical Chemistry
Indian Institute of Science, Bangalore - 560 012, India.

Abstract

Nanodendritic Pd electrodeposited on the poly(3,4-ethylenedioxythiophene) (PEDOT) modified Pd nanodendrite electrodes have been studied for electroanalysis of As(III) in 1 M HCl solution. The Pd nanodendrites are grown on a porous thin film of PEDOT by electrodeposition process. Pd-PEDOT/C electrodes are characterized by physicochemical and electrochemical studies. Cyclic voltammetry studies show that Pd-PEDOT/C electrodes exhibit greater electrocatalytic activity towards As(III)/As(0) redox reaction than the Pd/C electrodes. Differential pulse anodic striping voltammetry (DPASV) is performed for analysis of As(III) ion at pH 1.0. The PEDOT modified Pd electrode is highly sensitive towards As(III) detection with sensitivity of 1482 μA cm^{-2} μM^{-1}. A wide detection range up to 10 μM and low detection limit of 7 nM (0.52 ppb) are obtained with a pre-deposition time of 120 s under optimum conditions. High sensitivity and low detection limit obtained on PEDOT modified Pd, for the first time in the literature, are attractive from practical view point. Interference studies of Cu(II) ions are investigated and it is observed that Cu(II) ions do not interfere.

Keywords: Electroanalysis; Pd nanodendrites; poly(3,4-ethylenedioxythiophene); differential pulse voltametry; arsenic

*Corresponding author; e-mail: muni@ipc.iisc.ernet.in; Tel: +91-80-2293 3183

1. Introduction:

Arsenic occurs as an element in the earth crust. It also exists in a range of oxidation states from -3 to +5 *i.e.,* -3 (arsine), 0 (arsenic), +3 (arsenite) and +5 (arsenate)[1] and it is commonly present as oxyacids of As(III) and As(V) in groundwater. However, oxyacids of As(III) are more mobile and soluble than As(V).[2] Furthermore, the toxicity of As(III) is 50 times higher than As(V) due to its reactivity toward enzymes in human metabolism.[3-5] Chronic arsenic poisoning (arsenicosis) from drinking water has become a serious threat to human health worldwide. Symptoms of arsenic poisoning include headache, confusion, severe diarrhoea, nausea, vomiting, partial paralysis, blindness, skin lesions and drowsiness. Prolonged exposure to arsenic induces anomalies, cardiovascular and peripheral vascular disease, hematological disorders, carcinoma, lung fibrosis, keratosis and stillbirth. Furthermore, death can occur at high doses of arsenic exposure.[4] The World Health Organisation (WHO) recommends that arsenic in drinking water should be below 10 ppb (0.01 mg L^{-1}).[6] Several techniques have been applied for determination and quantification of arsenic and its compounds at trace levels, which include atomic adsorption spectrometer,[7] atomic fluorescence spectrometer,[8] inductively coupled plasma mass spectrometer[9] and fluorescence spectrometer.[10] Although, these techniques are used for arsenic analysis at picogram to nanogram levels, they require sample pre-treatment, expensive equipments, and high analytical cost. However, electroanalytical techniques are relatively widespread due to their portability, high sensitivity, low cost, high accuracy and also suitable for in-situ and real-time analysis.[11-13]Among the various electroanalytical techniques, stripping voltammetry is used for detection of As at different electrodes, which include hanging mercury drop electrode [14,15]and gold electrode.[16] Recently, an effective sensing of As was reported at electrodes made of surface modified nanosized materials.[17-24] Penner *et al.,*[25] reported that

nano/ultramicro sized ensembles delivered significantly high ratio of faradic to capacitive currents in relation to the conventional macro sized materials. The nanostructured materials exhibit many advantages such as higher surface area, higher mass transport, lower detection limit and greater signal to noise ratio than the corresponding bulk materials.[25, 26] It is know that, a thin film of conducting polymer (CP) modified electrode provides an uniform dispersion of metal nanoparticles, and thus enhances the catalytic activity, sensitivity and surface area of metal nanoparticles.[27] Moreover, a large surface to volume ratio allows lower detection limit and easy renewal of the surface with anti-fouling properties.[28-30] The composites of metal nanoparticles and CPs exhibit significant enhancement in sensing and catalytic activity.[31-35]

From a study of the above literature, it is understood that CPs modified nanomaterials exhibits greater activity for electroanalysis of organic/inorganic species than the unmodified materials. To the best of authors' knowledge, there are no reports on electrodeposition of 3-D nanodendrites of Pd on electrochemically prepared poly(3,4-ethylenedioxythiophene) (PEDOT) surface for As analysis. In the present work, electrodeposition of Pd nanodendrites on the surface of PEDOT coated carbon paper electrode is studied for As(III) detection, for the first time. Differential pulse voltammetric response of Pd-PEDOT/C electrode is highly selective towards detection of As(III) in comparison with Pd/C electrode. It is shown that there is a positive influence of PEDOT under-layer for Pd on electroanalysis of As(III). The determination of As(III) using this approach has the following advantages: easy synthesis, reproducibility, high stability, high sensitivity, high selectivity, and low detection limit. Results of these studies are reported.

2. Experimental

All analytical grade or high purity chemicals, namely, 3,4-ethylene dioxythiophene (EDOT) (Aldrich), $PdCl_2$ (Aldrich), As_2O_3 (Aldrich), H_2SO_4 (Merck), HCl (Merck), sodium

dodecyl sulphate (SDS) (Merck) and $CuSO_4$. $5H_2O$ (Merck) were used as received. All aqueous solutions were prepared using double distilled water. For the electrodeposition of PEDOT and Pd, a Toray carbon paper (thickness: 0.2 mm) was used as the current collector. A foil of 0.7 cm width and 3 cm length was sectioned out of a carbon paper sheet and 1.4 cm^2 at one end was exposed to the electrolyte. The rest of its part was used for electrical contact through a Cu wire and the unexposed area was masked completely by an insulating PTFE tape. An electrochemical glass cell of about 50 ml capacity, which had provision for introducing a working electrode, two Pt foil electrodes and a saturated calomel reference electrode (SCE) was used for the electrochemical studies. All the electrode potentials are reported with respect to SCE. The electrodepositions of thin film of PEDOT and Pd were carried out as reported previously.[36,37] The electrochemical deposition of PEDOT on bare carbon paper electrode was carried out at 0.90 V from a solution consisting of 10 mM EDOT + 10 mM SDS + 0.1 M H_2SO_4.[36] For Pd deposition, an electrolyte of 5 mM $PdCl_2$ + 0.1 M HCl was used and the deposition of Pd was carried out at 0.10 V.[37] For all experiments, Pd was deposited by passing a charge of 357 mC cm^{-2}, which corresponded to 0.2 mg cm^{-2} of Pd. The Pd electrodes were prepared with and without PEDOT on carbon paper for comparative studies.

As(III) stock solution (1 mM) was prepared from As_2O_3, which was prepared by dissolving arsenic(III) oxide in 1 M HCl. The surface morphology of Pd-PEDOT/C electrodes was characterized by FEI Company scanning electron microscope (SEM) model Sirion. Potentiostatic deposition of PEDOT and Pd and the electrochemical characterization studies were carried out using Solartron electrochemical interface model SI 1287 and Bio-logic potentiostat model VSP. The sensitivity of As(III) ion on Pd-PEDOT/C and Pd/C electrodes surface was measured with differential pulse anodic stripping voltammetric (DPASV) method. All experiments were conducted in an air conditioned room at 22 ± 1°C.

3. Results and discussion:

3.1. Physicochemical characterization studies:

The formation of face centered cubic crystalline Pd on both bare carbon paper and PEDOT coated carbon paper was studied by X-ray diffraction.[37] The SEM micrographs of electrodeposited Pd on carbon paper with and without PEDOT under-layer are shown in Fig. 1. Pd deposited on PEDOT/C is seen as a well oriented 3d-tree like nanodendritic morphology (Fig. 1(a)). The dendrites consist of several sub-dendrites with different dimensions (Fig. 1(a) inset). The dimensions of Pd nanodendrites are in the range from 500 nm to 6 μm. In contrast, the Pd particles deposited on bare carbon electrode are highly compact, triangular in shape and non-dendritic in morphology (Fig. 1(b)). The porous surface of electrodeposited PEDOT film on carbon paper electrode provides a large number of surface defects. From cyclic voltammetry, it was found that Pd deposition occurs at 0.35 V in the electrolyte of 5 mM $PdCl_2$ + 0.1 M HCl.[37] Therefore, the deposition of Pd was carried out at 0.10 V. The conditions of high overpotential (*i.e.,* 0.25 V) and low concentration of Pd salt facilitate electrocrystallization of Pd crystals and their further growth as Pd nanodendrites on the defect sites of PEDOT/C surface. The performance of a catalyst primarily depends on its active surface area. The electrochemical active surface area of Pd-PEDOT/C and Pd/C electrodes was measured by CO adsorption followed by oxidative striping method.[37] The area of nanodendritic Pd-PEDOT/C electrode was 84 cm^2 per 1 cm^2 geometric area of the electrode which was almost 10 times higher than that of non-dendritic Pd/C electrode (8.6 cm^2 per 1 cm^2), although the electrochemical deposition conditions were identical for both

the electrodes.[37] Therefore, the highly branched nanodendritic Pd possesses greater electrochemical active surface than the non-dendritic Pd/C electrode.

3.2. Electrochemical characterization studies:

The electrochemical response of Pd-PEDOT/C and Pd/C electrodes was studied by cyclic voltammetry. Typical cyclic voltammograms of carbon paper, PEDOT/C, Pd/C and Pd-PEDOT/C electrodes recorded in 0.1 mM As_2O_3 + 1 M HCl in the potential range of 0.40 to -0.20 V are shown in Fig. 2. As shown in Fig. 2 (i) and (ii), the voltammograms of bare carbon paper and PEDOT/C paper electrodes do not exhibit any redox current peaks within the potential window. Similar voltammograms were recorded for higher concentrations of As(III) in 1 M HCl electrolytes. Thus, these electrodes are electrochemically inactive for As(III) detection. The characteristics of voltammograms for Pd/C and Pd-PEDOT/C electrodes are qualitatively similar (Fig. 2 (iii) and (iv)). In the forward sweep from 0.40 to -0.20 V, a reduction peak (P_c) appears at -0.01 V for both Pd/C and Pd-PEDOT/C electrodes, which is attributed to the reduction of As(III) ions to As on Pd surface. In the reverse sweep, an intense oxidation peak (P_a) is observed at 0.18 V. This is due to the re-oxidation of As to As(III). It is clear that As(III) undergoes reduction on Pd surface but not on PEDOT surface (Scheme 1). Furthermore, the peak current density (both cathodic and anodic) on Pd-PEDOT/C electrode is about 8 times greater than those of Pd/C electrode, although the amount of charge used for Pd deposition is the same (357 mC cm^{-2}) in both cases. This is in agreement with the active surface area measured by CO stripping analysis. These results show that, the electroactive sites of nanodendritic Pd-PEDOT/C electrode are greater than Pd/C electrode, due to the presence of porous thin film of PEDOT layer. The defects on porous surface of PEDOT layer facilitate the formation of nanodendritic morphology of Pd on PEDOT/C electrode. These nanodendritic Pd layers possess high energy surface sites such as short branches, kinks, steps, edges, etc. The enhanced surface area of Pd deposited on

PEDOT favours in increased voltammetric currents for reduction of As(III) followed by the oxidation of As(0).

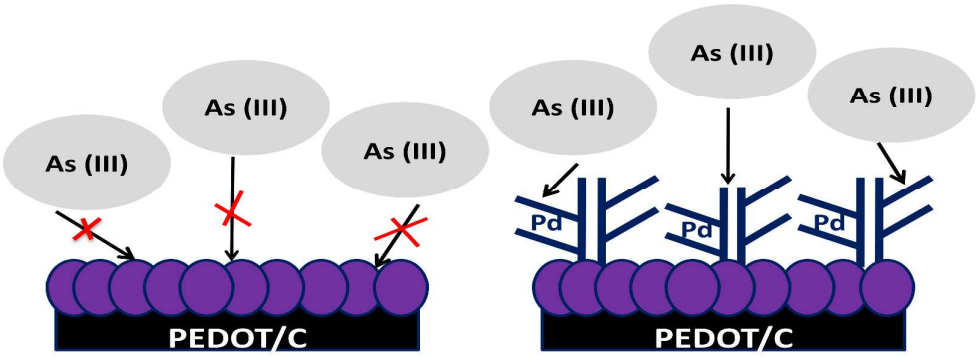

Scheme 1: *Schematic representation of As(III) ions adsorbed on the surface of Pd nanodendrities on PEDOT coated carbon paper .*

Cyclic voltammograms of Pd-PEDOT/C electrode were recorded at different sweep rates in 0.1 mM As_2O_3 + 1 M HCl electrolyte (Fig. 3(a)). It is observed that peak current densities (j_p) for both reduction peak (P_c) and oxidation peak (P_a) increase with an increase in sweep rate. The oxidation peak potential (E_{pa}) shifts to more positive direction with increasing sweep rate. Considering a large peak potential separation (about 177 mV at 10 mV s^{-1} sweep rate) and a shift in peak potential with sweep rate, peak current density (j_p) is given by (1).

$$j_p = 2.99 \times 10^5 \, n \, (\alpha \, n')^{½} \, c \, D^{1/2} \, \upsilon^{1/2} \qquad (1)$$

where α is transfer coefficient, n' is number of electrons involved in the rate determining step, n is total no of electrons, c is concentration, D is diffusion coefficient and υ is sweep rate. Plots of j_{pa} and j_{pc} versus υ are shown as log-log plots in Fig. 3(b). The slopes of log j_{pa} and log j_{pc} versus log υ are close to 0.5 suggesting that the reactions are diffusion controlled.

The peak potential for an irreversible reaction is proportional to log υ and (dE / dlog υ) is related to (α n'). [38]

$$(dE / d\log \upsilon) = 0.0296 / (\alpha n') \quad (2)$$

The dependence of peak potentials of forward peak (E_{pa}) on log υ is shown in Fig. 3(c). From the slope of E_{pa} versus log υ (0.026 V), the value of transfer coefficient (α) obtained is 0.38, assuming n' = 3 for electrooxidation of As to As(III).

3.3. Electroanalytical detection of As(III):

For the purpose of trace analysis of As(III), As was first electrodeposited potentiostatically on Pd-PEDOT/C electrodes and then differential pulse voltammetry was employed to oxidize As to As(III). Anodic stripping differential voltammogram (ASDPV) recorded in 1 μM As_2O_3 + 1 M HCl after pre-deposition of As at -0.30 V for 120 s is shown in Fig. 4(a). For the ASDPV experiment, pulse amplitude of 30 mV, pulse width 0.2 s, pulse period of 0.6 s and potential increment of 4 mV were employed. A reproducible current peak appears at 0.20 V (Fig. 4(a) i) and such current peak is absent in the 1 M HCl in the absence of As_2O_3 (Fig. 4(a) ii). Several experiments were conducted to arrive at optimum conditions of pre-deposition of As by varying the deposition potential and time. The effect of deposition potential on DPV current is shown in Fig. 4(b). A maximum and nearly the same DPV current are measured when the deposition potential is between -0.50 V and -0.30 V. There is decrease in DPV current when the deposition potential is increased from -0.30 V to 0.0 V. At potential more negative to -0.30 V, the DPV signal became noisy and irreproducible due to the interference of hydrogen evolution reaction on Pd. Therefore, -0.30 V was chosen for the pre-deposition of Pd. At -0.30 V, the deposition time was varied from 10 to 250 s and the variation of DPV current on time is presented in Fig. 4(c). There is a linear increase in DPV current with an increase in deposition time up to about 150 s and the current is nearly

constant thereafter. As a result of these experimental studies, -0.30 V and 120 s were chosen as As pre-deposition potential and time, respectively, before subjecting Pd-PEDOT/C electrode for ASDPV.

ASDPV voltammograms of a Pd-PEDOT/C electrode recorded in 1 M HCl with different concentrations of As_2O_3 are presented in Fig. 5(a). There is an increase of DPV current with an increase in concentration of As_2O_3 (Fig. 5(b)). There is a linear increase in current with an increase in concentration of As(III) with low detection limit of 0.007 μM (0.52 ppb) and signal to noise ratio of 3 (Fig. 5(b)). The value of R^2 is 0.9998 indicating an excellent linear fit of the experimental data. The slope of the linear plot (Fig. 5(b)) obtained for Pd-PEDOT/C electrode is 1482 μA cm^{-2} μM^{-1}. Thus the sensitivity of the electrode for As(III) detection is very high. For comparison, ASDPV data of Pd/C electrode are shown in Fig. 5(c). The increase of DPV current with concentration of As_2O_3 is linear with a low detection limit of 3 μM, R^2 of 0.9988 and sensitivity of 0.84 μA cm^{-2} μM^{-1}. Thus, Pd-PEDOT/C electrode is several times superior to Pd/C electrode in terms of low detection limit and sensitivity.

Electroanalysis primarily requires a fast adsorption of the analyte and electron transfer process, which are facilitated by multiple active sites on the electrode. The above observed results of superior performance of Pd-PEDOT/C electrode are due to the nanodendritic structure of Pd with larger surface to volume ratio. The multiple active sites on Pd nanodendrites play key role for fast adsorption of As(III) ions and the nanodendrites also act as nanoscale bridges between the electrode surface and PEDOT/C substrate.[39] As a result, the sensitivity of Pd-PEDOT/C electrode is greater than that of Pd/C electrode for detection of As(III) ions in acidic media. The values of detection limit and sensitivity of PEDOT modified Pd nanodendritic electrode are compared with reported values in Table 1. As seen in Table 1, 1985 μA cm^2 μM^{-1} is the best sensitivity value reported till now for As(III) ion detection by

AuNPs/CNT electrode.[17] The value obtained in the present study on nanodendritic Pd-PEDOT/C electrode i.e. 1482 μA cm^{-2} μM^{-1}, is superior to various reported values (Table 1). Furthermore, the low detection limit estimated is 0.007μM (7 nM), which is much lower than the recommended level of 0.13 μM (10 ppb) by WHO. Thus, the above results demonstrate that the nanodendritic Pd-PEDOT/C electrode is useful for As(III) detection with a very high sensitivity and very low detection limit in acidic media.

The stability and the electroanalytic activity of Pd-PEDOT/C and Pd/C electrodes were examined in 0.1 mM As_2O_3 + 1 M HCl solution by repeated cyclic voltammetry. The experiment was performed at a sweep rate of 50 mV s^{-1} for 100 cycles. The anodic peak current density (j_{pa}) on Pd/C electrode increases gradually fairly up to 0.85 mA cm^{-2} at the 25th cycle (Fig. 6(i)). After 25th cycle, the anodic peak current density value decreases gradually and reaches a value of 0.73 mA cm^{-2} at 100th cycle, which is about 85 % of that 25th cycle (Fig. 6(ii)). The anodic peak current density of Pd-PEDOT/C electrode shows an increase from 0.8 mA cm^{-2} to 1.86 mA cm^{-2} at 80th cycle. Subsequently, it remains nearly constant. At 100th cycle, the value of is 97% of the 80th cycle. This result demonstrates that, Pd-PEDOT/C electrode retains its activity towards the detection of As(III) without undergoing poisoning due to any intermediate species adsorbed during the oxidation process. Thus, the Pd-PEDOT/C electrode exhibits superior performance than that Pd/C.

3.4. Interference studies:

A main drawback of As(III) detection using ASDPV method is that some interference species, which can be reduced together with As(III) and then undergo oxidation during the stripping process near the oxidation potential of As. Cu(II) is known as a common interfering ion in water, which affects the detection of As(III).[43] During the predeposition step Cu interacts with As and forms a inter-metallic compound (Cu_3As_2) as well as Cu metal.[19] Cyclic

voltammetry experiment was carried out to evaluate the interference effect of Cu(II) species. Cyclic voltammograms were recorded after five additions of Cu(II) at Pd-PEDOT/C electrode in 1 M HCl containing 0.1 mM As(III) (Fig. 7). As shown in Fig. 7, a reduction peak appeared at -0.30 V, which is attributed the reduction of Cu(II) to Cu. On the reverse anodic sweep, an oxidation peak (Pa) observed at 0.17 V, which is due to the subsequent reoxidation of Cu to Cu(II). The peak current density of a pair of redox peaks at -0.30 V and 0.17 V is increased with each addition of Cu(II). However, the oxidation peak current density of As(III) at 0.23 V is unchanged. These result demonostrates that the Cu(II) does not have any interference effect to the oxidation of As(III) on Pd-PEDOT.

4. Conclusions:

The PEDOT modified Pd nanodendrite electrodes were studied for electroanalysis of As(III) in 1 M HCl solution. The Pd nanodendrites were grown on a porous thin film of PEDOT by electrodeposition process. Pd-PEDOT/C electrodes were characterized by physicochemical and electrochemical studies. Cyclic voltammetry studies showed that Pd-PEDOT/C electrodes exhibited greater electrocatalytic activity towards arsenic redox reaction than the Pd/C electrodes. Differential pulse anodic striping voltammetry (DPASV) was performed for analysis of As(III) ion at pH 1. The PEDOT modified Pd electrode was highly sensitive towards As(III) detection with sensitivity of 1482 $\mu A\ cm^{-2}\ \mu M$. A wide detection range up to 10 μM and low detection limit of 7 nM (0.52 ppb) were obtained with a pre-deposition time of 120 s under optimum conditions. Interference studies of Cu(II) ion was investigated and it was observed that Cu(II) ions did not show any significant interference effect. Thus, a high sensitivity and a low detection limit obtained with Pd-PEDOT/C electrodes are very attractive for practical use of these electrodes for As(III) detection.

References:

1. M. M. F. Morel, A.M.L. Kraepiel and M. Amyot, *Annu. Rev. Ecol. Syst.,* 1998, **29**, 543.

2. L. E. Deuel and A. R. Swoboda, *J. Environ. Qual.,* 1972, **1**, 317-320.

3 L. Vega, M. Styblo, R. Patterson, W. Cullen, C. Wang and D. Dermolec, *Toxicol. Appl. Pharmacol.,* 2001, **172**, 225-232.

4. B. K. Mandal and K. T. Suziki, *Talanta*, 2002, **58**, 201-235.

5. R. S. Stojanovic and A. M. Bond, *Anal. Chem.,* 1990, **62**, 2692-2697.

6. A. H. Smith, E. O. Lingas and M. Rahman, *Bull. WHO*, 2000, **78**, 1093-1103.

7. P. Niedzielski, *Anal. Chim. Acta*, 2005, **551**, 199-206.

8. G. Ma, W. B. Xie, J. Liu, X. Y. Li and Y. W. Jin, *Spectrosc. Spectr. Anal.,* 2007, **27**, 807.

9. P. Wang, G. Zhao , J. Tian and X. Su, *J. Agric. Food Chem.*, 2010, **58**, 5263-5270.

10. Y. M. Huang and C. W. Whang, *Electrophoresis.,* 1998, **19**, 2140-2144.

11. R. Feeney and S.P. Kounaves, *Anal.Chem.,* 2000, **72**, 2222-2228.

12. A. O. Simm, C. E. Banks and R.G. Compton, *Anal. Chem*., 2004, **76**, 5051-5055.

13. X. Dia, G. G. Wildgoose, C. Salter, A. Crossely and R. G. Compton, *Anal. Chem*., 2006, **78**, 6102.

14. L. Meites, *J. Am. Chem. Soc.,* 1954, **76**, 5927-5931.

15. A. Profumo, D. Merli and M. Pesavento, *Anal. Chim. Acta*, 2005, **539**, 245-250.

16. R. Feeney and S. P. Kounaves, *Talanta*, 2002, **58**, 23-31.

17. L. Xiao, G. W. Wildgoose and R. G. Compton, *Anal. Chim. Acta*, 2008, **620**, 44-49.

18. B. K. Jena and C. R. Raj, *Anal. Chem*., 2008, **80**, 4836-4844.

19. S. S. Mendez, O. D. Renedo and M. J. A. Martinez, *Electroanal.*, 2009, **21**, 635-639.

20. A. Salimi, H. Mamkhezri, R. Hallaj and S. Soltanian, *Sens. Actuators B*, 2008, **129**, 246-254.

21. X. Dai, O. Nekrassova, M. E. Hyde and R. G. Compton, *Anal. Chem.,* 2004, **76**, 5924-5929.

22. Q. X. Zhang and L. B. Yin, *Electrochem. Commu.,* 2012, **22**, 57–60.

23. X. Dai and R. G. Compton, *Analyst*, 2006, **131**,516-521.

24. D. Li, J. Li, X. Jia, Y. Han and E. Wang, *Anal. Chim. Acta*, 2012, **733**, 23-27.

25. R. M. Penner and C. R. Martin, *Anal. Chem.,* 1987, **59**, 2625-2630.

26 H. Reller, E. Kirowa-Eisner and E. Gileadi, *J. Electroanal. Chem*., 1984, **161**, 247-268.

27. N. F. Atta and M. F. E. Kady, *Sens. Actuators B,* 2010, **145,** 299–310.

28. S. K. Das, Md. M. R. Khan, T. Parandhaman, F. Laffir, A. K. Guha, G. Sekaran and A. B. Mandal, *Nanoscale*, 2013, **5**, 5549-5560.

29. S. Y. Lee, H. J. Kim, R. Patel, S. J. Im, J. H. Kim and B. R. Min, *Poly. Adv. Tech.,* 2007, **18**, 562-568.

30. C. G. Caridade, C. M. A. Brett, *Curr. Anal. Chem.,* **2008**, *4,* 206-214.

31. M. Giannetto,G. Mori, F. Terzi, C. Zanardi and R. Seeber, *Electroanal.,* 2011, **23**, 456 – 462.

32. S. Anandhakumar, J. Mathiyarasu, K. L. N. Phani, V. Yegnaraman*, J. Anal. Chem.,* 2011, 2, 470-474.

33. H. Yamato, M. Ohwa and W. Wernet, *J. Electroanal. Chem.,* 1995, **397**, 163-170.

34. M. Heitzmann, L. Basaez, F. Brovelli, C. Bucher, D. Limosin, E. Pereira,B. L. Rivas, G. Yal, E. S. Aman and J-C Moutet, *Electroanal.*, **2005**, 17, 1970 – 1976.

35. S. Dash and N. Munichandraiah , *ECS Electrochem. Lett.,* 2013, **2**, B17- B20.

36. S. Dash and N. Munichandraiah, *J. Appl. Electrochem.,* 2012, **42**, 59-67.

37. S. Dash and N. Munichandraiah, *Electrochim. Acta*, 2012, **80**, 68-76.

38. R. Greef, R. Peat, L. M. Peter, D. Pletcher, J. Robinson, Instrumental Methods in Electrochemistry, Ellis Horwood Ltd. Chichster, London, **1985**, p.186

39. X. Wen, Y.T. Xie, M. W. C. Mak, K. Y. Cheung, X. Y. Li, R. Renneberg and S. Yang, *Langmuir*, **2006,** *22,* 4836-4842.

40. N. A. Yusof, N. Daud, T. W. Tee and A. H. Abdullah, *Int. J. Electrochem. Sci.,* 2011, **6** 2385 – 2397.

41. T. A. Ivandini, R. Sato, Y. Makide, A. Fujishima and Yasuaki Einaga, *Anal. Chem*., 2006**, 78**, 6291-6298.

42. T. W. Hamilton and J. Ellis, Anal. *Chim. Acta,* 1980, **119,** 225-233.

43. H. M. Anawar, J. Akai, K. M. G. Mostofa, S. Safiullah, S. M. Tareq, *Environ. Int.,* 2002, **27**, 597– 604.

Figure captions

Fig. 1: SEM micrographs of **(a)** Pd–PEDOT/C electrode (magnification: 50,000 x) and **(b)** Pd/C electrode (magnification: 50,000 x). **Inset:** SEM micrograph of Pd-PEDOT/C electrode at higher magnification (1, 00, 000 x). (Pd deposition charge: 357 mC cm^{-2} (geometric area)).

Fig. 2: Cyclic voltammograms of carbon paper (i), PEDOT/C (ii), Pd/C (iii) and Pd-PEDOT/C (iv) electrodes in 0.1 mM As_2O_3 + 1 M HCl at a sweep rate of 10 mV s^{-1}. Current density is calculated using geometric area of the electrode.

Fig. 3: **(a)** Cyclic voltammograms of Pd-PEDOT/C electrode in 0.1 mM As_2O_3 + 1 M HCl at sweep rates of 2 (i), 5 (ii), 10 (iii), 15 (iv), 20 (v), 25 (vi) and 30 mV s^{-1} (vii). **(b)** Peak currents verses sweep rate as log-log plots**. (c)** anodic peak current density verses anodic peak potential as a log-log plot. (Pd deposition charge: 357 mC cm^{-2}; current density is calculated using geometric area of the electrode).

Fig. 4: (a) Differential pulse voltammograms of a Pd-PEDOT/C electrode after deposition of As at -0.30 V for 120 s in 1μM As(III) in 1 M HCl and effect of the **(b)** pre-deposition potential (constant time: 120 s) and **(c)** pre-deposition time (constant potential: -0.30 V) on differential pulse peak currents response of 1 μM As(III) in 1 M HCl at Pd-PEDOT/C electrode.

Fig. 5: (a) DPASV curves of Pd-PEDOT/C electrode in 1 M HCl (i) and in different concentration (from 0.01 to 0.16 μM) of As (III) + 1 M HCl (ii) and DPASV calibration plots of peak current density versus arsenic concentration at **(b)** Pd-PEDOT/C and **(c)** Pd/C

electrodes. (pre-deposition at -0.30 V for 120 s). Current density is calculated on the basis of geometric area (1.4 cm^2).

Fig. 6: Cyclic voltammetric anodic peak current density (j_{pa}) versus number of repetitive cycles for Pd/C (i) and Pd-PEDOT/C (ii) electrodes in 0.1 mM As_2O_3 + 1 M HCl. Sweep rate: 50 mV $s^{-1.}$ Current density is calculated on the basis of geometric area (1.4 cm^2).

Fig. 7: Cyclic voltammograms of Pd-PEDOT/C electrode in 0.1 mM + 1 M HCl with different concentrations of Cu(II) ion. Current density is calculated using geometric area of the electrode.

Table 1: Electroanalysis of As(III) using different electrode and techniques from the literature survey (LC: liquid chromatography, FIA: flow injection analysis, LSV: linear sweep voltammetry, CV: cyclic voltammetry, ASV: anodic stripping voltammetry, SWV: square wave voltammetry, SPCE: screen printed carbon electrode, GCE: glassy carbon electrode, CNT: carbon nanotube, BDD: boron doped diamond electrode and NPs: nanoparticles)

Working electrode	**Technique**	**LOD (ppb)**	**Sensitivity ($\mu A\ cm^{-2}\ \mu M^{-1}$)**	**Reference**
Pt	LC	14.9	--	[5]
PtNPs/SPCEs	CV	5	--	[19]
CNT/Glutamine/Nafion modified Pt	ASDPV	2.7	100	[40]
PtNPs/GCE	CV	2.1	0.21	[23]
Ir-BDD	FIA	1.5	0.43	[41]
CoNPs-GCE	Amperometry	0.83	0.111	[20]
Au film-GCE	ASV	0.56	--	[42]
AuNPs-GCE	SWV-LSV	0.014	95	[21]
AuNPs/CNT	SWV	0.1	1985	[17]
Pd-PEDOT/C	ASDPV	0.53	1482	Present work

Fig. 1

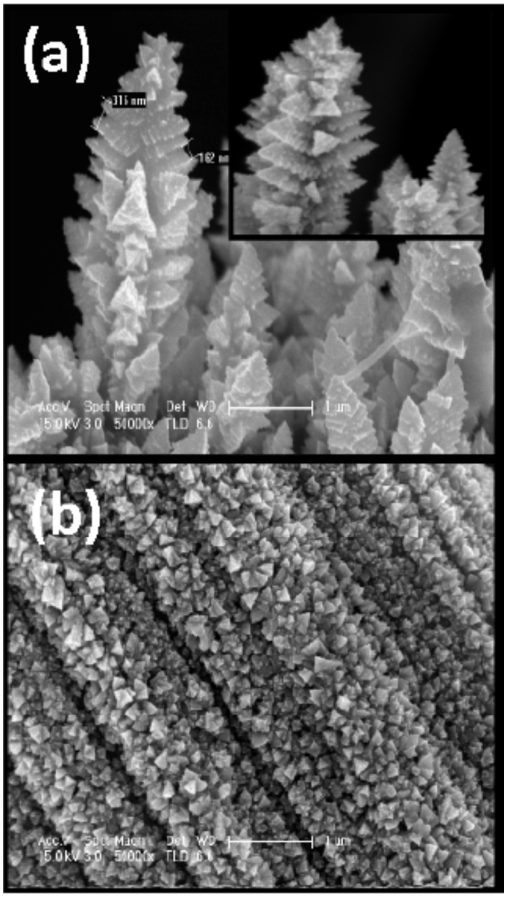

Fig. 2

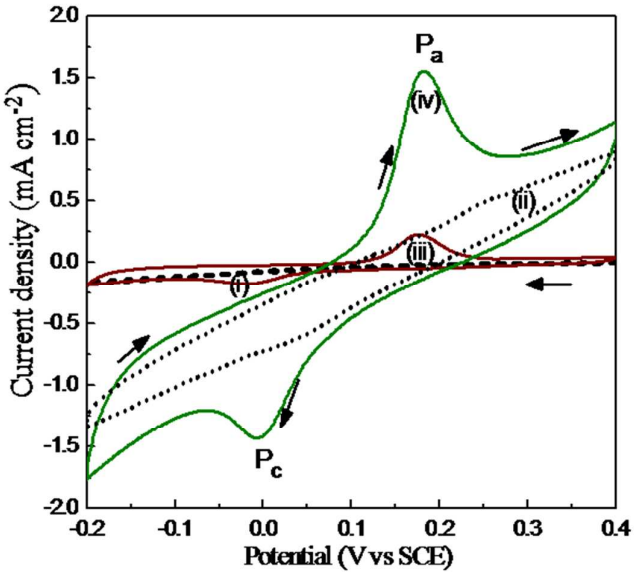

Fig. 3

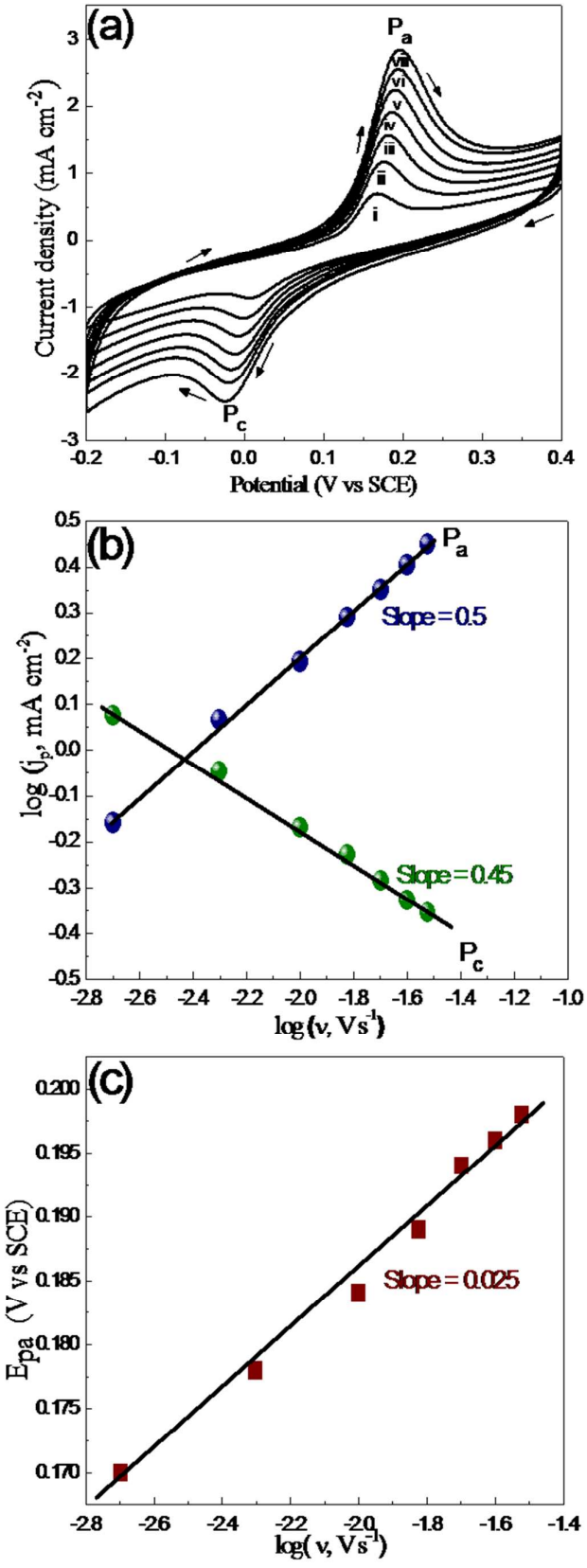

Fig. 4

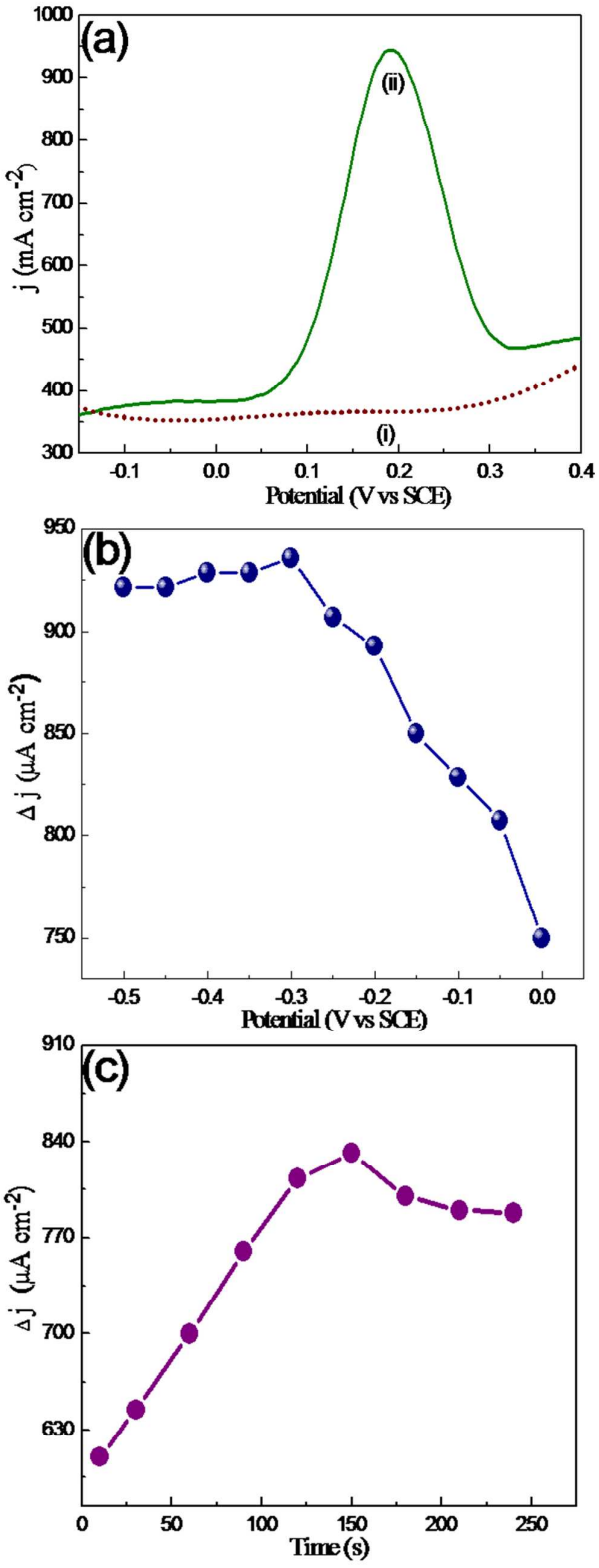

Fig. 5

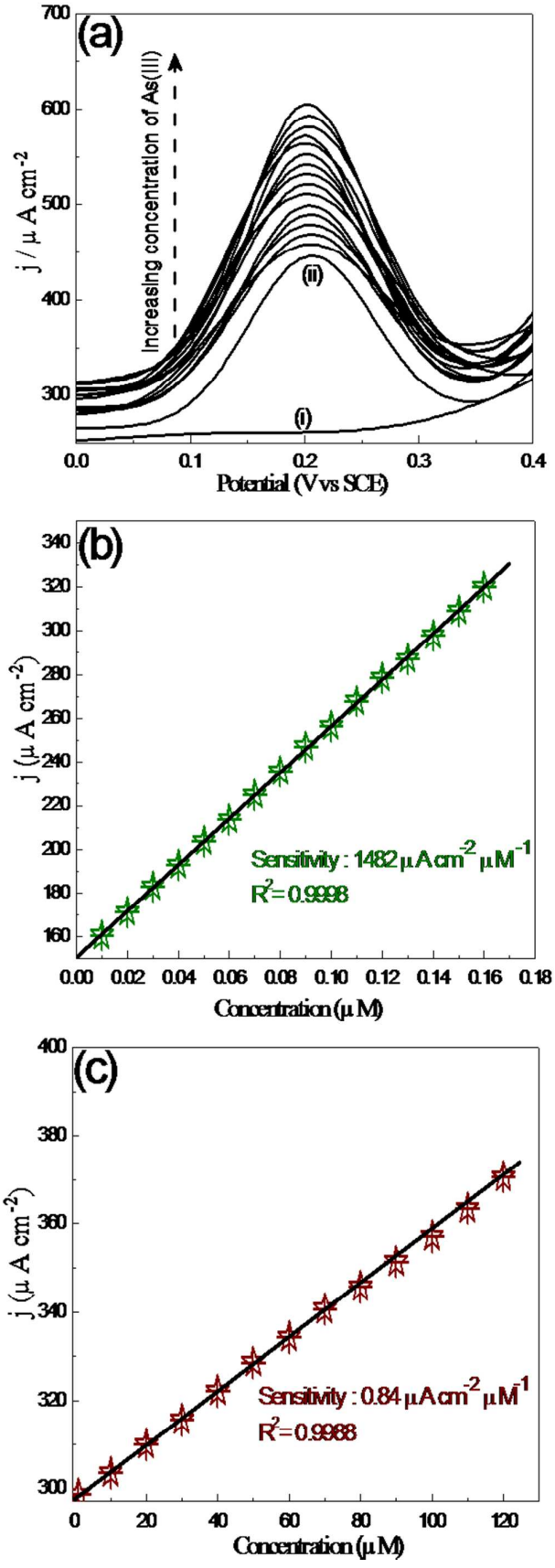

Fig. 6

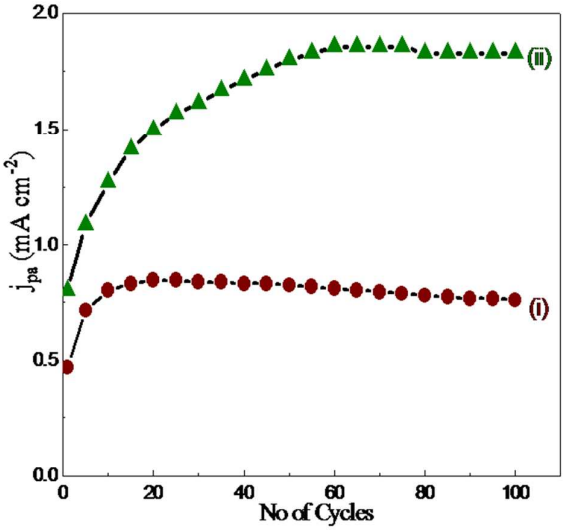

Fig. 7

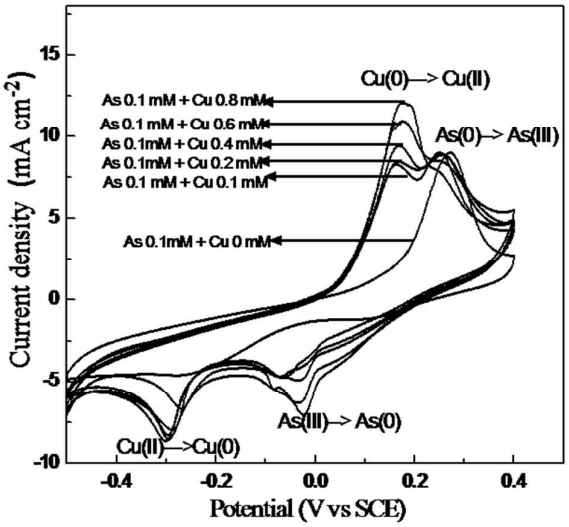

TOC